Thermal design and analysis of a multi-stage 30 K radiative cooling system for EPIC

Talso Chui, Jamie Bock, Warren Holmes and Jeff Raab*

Jet Propulsion Laboratory, California Institute of Technology and * Northrop Grumman Aerospace Systems.

The Experimental Probe of Inflationary Cosmology (EPIC) is an implementation of the NASA Einstein Inflation Probe mission, to answer questions about the physics of Inflation in the early Universe by measuring the polarization of the Cosmic Microwave Background (CMB). The mission relies on a passive cooling system to cool the enclosure of a telescope to 30 K; a cryocooler then cools this enclosure to 18 K and the telescope to 4 K. Subsequently, an adiabatic demagnetization refrigerator further cools a large focal plane to ~100 mK. For this mission, the telescope has an aperture of 1.4 m, and the spacecraft's symmetry axis is oriented ~45 degrees relative to the direction of the sun. The spacecraft will be spun at ~0.5 rpm around this axis, which then precesses on the sky at 1 rph. The passive system must both supply the necessary cooling power for the cryocooler and meet demanding temperature stability requirements. We describe the thermal design of a passive cooling system consisting of four V-groove radiators for shielding of solar radiation and cooling the telescope to 30 K. The design realizes loads of 20 and 68 mW at the 4 K and 18 K stages on the cooler, respectively. A lower cost option for reaching 40 K with three V-groove radiators is also described. The analysis includes radiation coupling between stages of the radiators and sunshields, and parasitic conduction in the bipod support, harnesses, and ADR leads. Dynamic effects are also estimated, including the very small variations in temperature due to the scan motion of the spacecraft.

1. Introduction

This paper describes the thermal design of the sunshield and passive radiator for the EPIC mission [1]. Passive radiative cooling makes use of deep space as a low temperature reservoir to sink heat from a spacecraft. When solar system dust and star lights are taken into account, the effective temperature of the sky is approximately 7 K [2]. This provides a large temperature difference from ambient (~300 K) for heat rejection and cooling. Radiative cooling has been successfully applied to solve cooling needs of many previous missions, the latest of which are the Spitzer Space Telescope and the recently-launched Planck CMB anisotropy mission. The V-Groove radiator design of EPIC follows the footsteps of the Planck mission [3]. It consists of multiple stages of radiators, each having a V-shape cross section. The angle of the "V" is progressively narrower from the outer sun-facing shield toward the inner and colder shields. Thermal radiations between two shields are guided into space by successive reflections at the low emissivity surfaces of the shields.

Two design options were explored - a four-shield design and a three shield design that would cool the Optical Box to 29 K and 36 K respectively. Figure 1a shows EPIC with the four-shield design. The first shield refers to the shield facing the sun. The three-shield version is the same except that the fourth shield is removed. Each shield in Figure 1a represents a doubled layered shield, which is needed to mitigate the risk of micro-meteorites puncturing the shield. The thermal effect of double-layering is included in the thermal design. Also shown in Fig. 1a is an Optical Box with the telescope inside, mounted on an Optical Bench. Figure 1c shows EPIC in the launch configuration. Figure 1c shows the solar illumination and the scan pattern of EPIC.

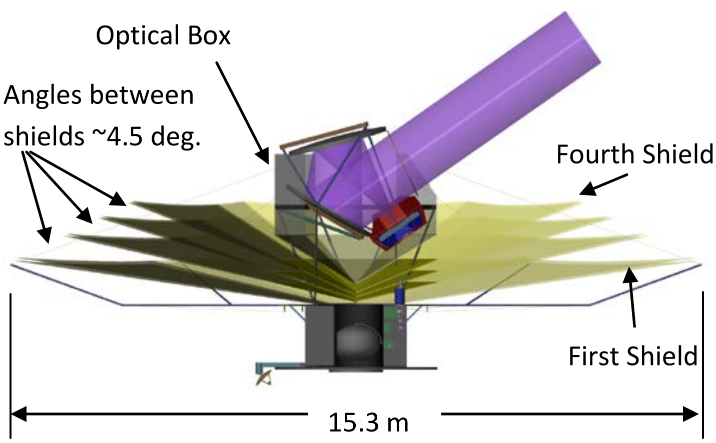

(b)

(a)

(c) 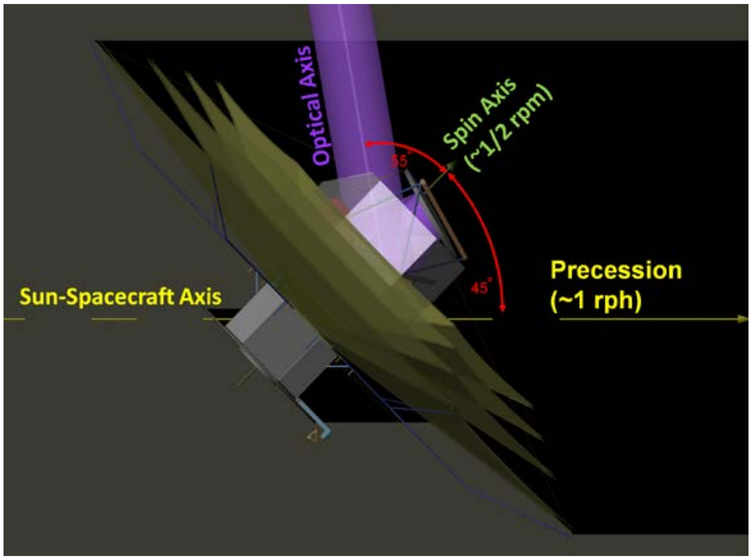

Figure 1: (a) EPIC with the four shields deployed. The overall dimensions and angles between the shields are also shown. (b) EPIC in the launch configuration; and (c) the solar illumination and the scan pattern.

2. Model Input

The overall geometry is based on a three dimensional CAD drawing of the conceptual design. A solar incident flux of 1327 W/m^2 is applied at an angle of 45 degrees relative to the symmetry axis of the spacecraft. Power is applied to the spacecraft's nominally room temperature radiators to simulate the total dissipation of electronic equipment. Power is also applied to simulate the total power dissipated at the Adiabatic Demagnetization Refrigerator (ADR), which is mounted on the cryogenic rejection stage of a four-stage cryocooler. Table I summarizes the thermal properties of materials used for the various components. The diameter and the thickness of the gamma-alumina main struts were derived by structural analysis of launch loads. Figure 2 summarizes the thermo-optical coating applied on various surfaces. The spacecraft surface and the sun-seeing side of the first shield is covered with silver Teflon for its low solar absorptivity and high infra-red emissivity, which help reject solar heat input. Table II summarizes the optical properties of these coatings. The temperature dependent emissivity of aluminized Kapton was inherited from a previous study for the SAFIR proposal [3]. The temperature dependent thermal conductivities of the materials used are plotted in Figure 3.

Table I: Summary of thermal properties at 300 K.

Components	**Material**	**Thermal conductivity** (W/m-K)	**Specific Heat** (J/kg-K)	**Density** (Kg/m^3)
Spacecraft	Aluminum 6061-T6	155.8 *	900	2702
Center piece of all sunshields	Honey comb panel modeled as 1 layer of Aluminum 6061-T6	155.8 *	900	2702
Deployable piece of sunshields	Kapton	0.12	1090	1420
Main Struts	Gamma-alumina tubes	1.8 *	900	2000
Mirrors and Focal Plane	Carbon fiber reinforced plastic (CFRP)	1 *	837	2000
Manganin Wires	Along struts	20 *	NA	NA
Gold shielding	Along strut. (99.9% purity, not annealed)	200 *	NA	NA
HTS wires	12 wires between the Optical Bench and the last shield. The length is 4 times the strut length along this section	$3.7T^{0.62}$	NA	NA
Brass leads connected to HTS Wires	24 wires along strut from the last shield outward	90 *	NA	NA
Teflon Insulations	Along the length of the strut	0.28 *	NA	NA

* Temperature dependent properties are used in the model.

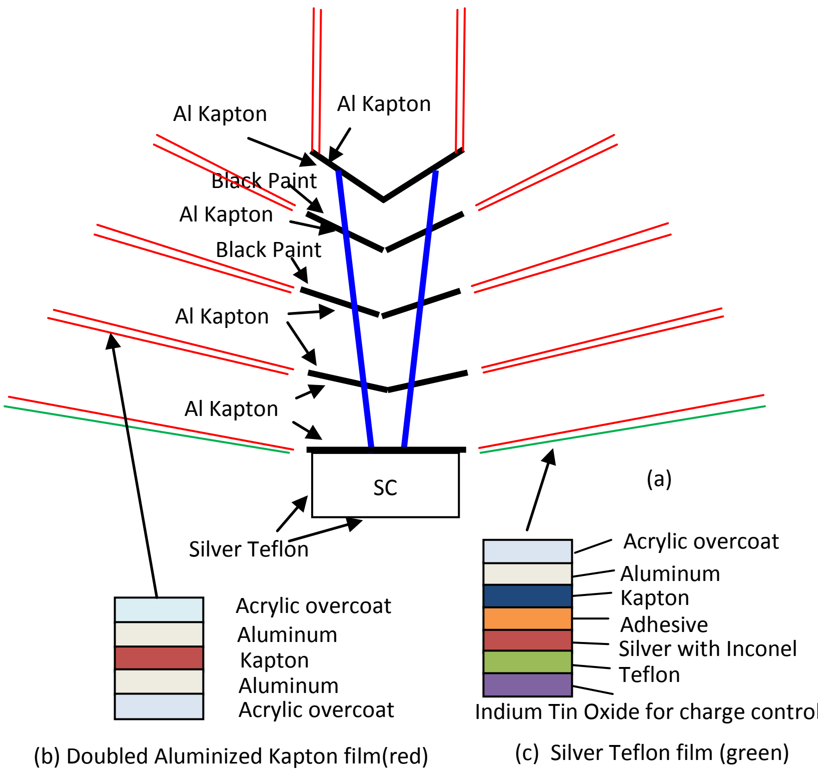

Figure 2: a) Optical coatings applied to components of EPIC. b) Red color line represents a double aluminized Kapton film. c) Green line represents a silver Teflon film.

Table II: Thermo-optical properties of coatings at 300 K from www.sheldahl.com.

Coating	Solar Absorptivity α	Infrared Emissivity ε	Specularity	Thermal Conductivity (W/m-K)
Silver Teflon	0.14	0.75	95%	NA
Aluminized Kapton	0.14	0.056 *	95%	NA
Black Paint	0.94	0.9	100%	NA
MLI	NA	Effective ε = 0.05	NA	$1.2\text{x}10^{-6}$

* Temperature dependent properties are used in the model.

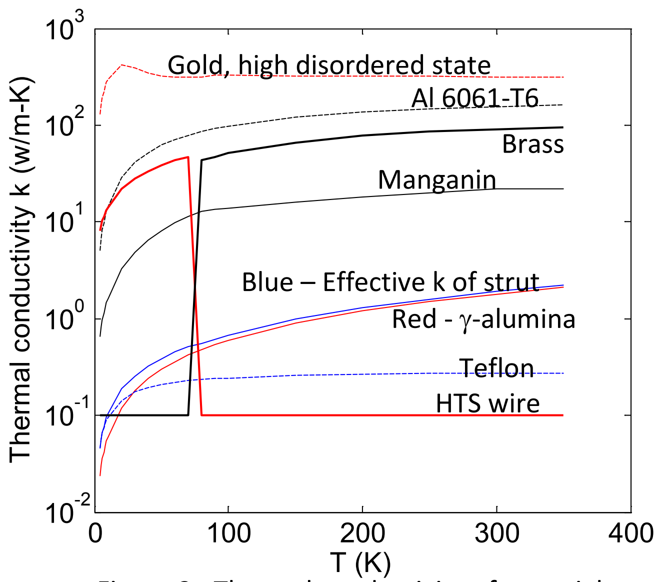

Figure 3: Thermal conductivity of material used

3. *Model Technique*

3.1 Tools

Thermal Desktop 5.1 is used for the model. Thermal Desktop is a graphical user interface that is built on top of a SINDA engine. It employs finite difference method to solve the heat equation in a sheet (2D geometry). 3D geometries are built by putting sheets together, and allowing thermal conduction to occur at the boundary of the sheets. Although true 3D heat flow can be treated by finite element method in Thermal Desktop, it is not used in the model because the problem being treated is primarily a radiative heat transfer problem, not a 3D heat flow problem. For radiative heat transfer, we use a module of Thermal Desktop called RADCAD which employs Monte Carlo ray trace technique to calculate the coupling between surfaces. The model ran on a PC with a 3.6 GHz Pentium-4 CPU and 4 GB of RAM.

3.2 Model Statistics

The model has 2900 nodes. For each node an average of 50,000 rays were shot for the Monte Carlo simulation. It took approximately 8 minutes to run.

3.3 Heat Conduction by Wires

It would be too laborious to input the geometry of each wire into the model. The approach taken is to increase the thermal conductivity of the struts by including the effect of heat conduction by all the wires. The effective conductivity is computed as: $k_{eff} = \sum \frac{k_i(A_i/L_i)}{(A_\gamma/L_\gamma)}$, where k_i, A_i and L_i are the thermal conductivity, the cross-section area and length of the wire and struts denoted by the subscript i, and L_γ and A_γ are the length and total cross-section areas of the gamma-alumina struts. The results are shown by the blue lines in Fig. 4. Figure 4 also shows that roughly 10% of conductive heat is carried by wires.

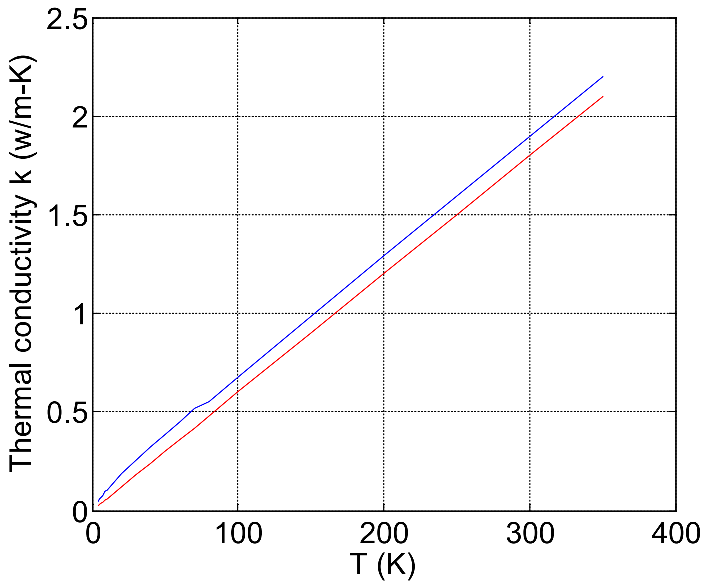

Figure 4: The thermal conductivity of gamma-alumina (red) and k_{eff} (blue).

<u>3.4 Double-Layer Shield</u>

Double-layer deployable shields are used for mitigation against the risk of micro-meteorites puncturing the shields. It also allows a temperature difference to develop from one layer to the other. Thermal Desktop allows the addition of a layer of MLI to simulate the effect of a double-layer shield. Mathematically, MLI is treated as a two-layer surface with an effective emissivity for the interior facing surfaces. We used an effective emissivity of 5% for modeling double-layer shields. The effect of radiation escaping between the layers is not treated, resulting in a conservative calculation.

4. Model Results

<u>4.1 Four- Shield Option, Cryocooler On</u>

With the cryocooler off, the model shows that the Optical Box reaches a temperature of 29 K and the optics inside reaches a temperature of 22 K. When the cryocooler is turned on, the Optical Box is cooled to 18 K by a thermal stage of the cryocooler connected to it. The Optical Bench is connected to the coldest stage of the cryocooler and is cooled to 4 K. The temperature of the Optical Bench as a function of cooling power is given in Table III. The shaded column gives the designed heat lifts and temperatures of the cryocooler for EPIC. A heat lift of 20.25 mW is required to keep the Optical Bench at 4 K with heat loads from the ADR, and 68 mW is required to keep the Optical Box Bottom at 18K. In the design of the cryocooler a heat load margin of 100% is applied to these estimates. Figure 5 and 6 are the color maps of EPIC and its telescope respectively. Table IV is the heat transfer summary between different thermal stages.

Table III: Cooling power at the Optical Bench versus temperature. The Optics Box Bottom is kept at 18 K. The shaded column is the requirement on the cryocooler.

Cooling power (mW)	0	10	15	18.5	20	20.25	20.5	21
Optical Bench T (K)	17.35	13.86	11.02	7.62	4.83	4.02	3.23	1.43
Optics Box Bottom P (mW)	78.2	74.0	71.4	69.1	68.0	67.8	67.5	67.0

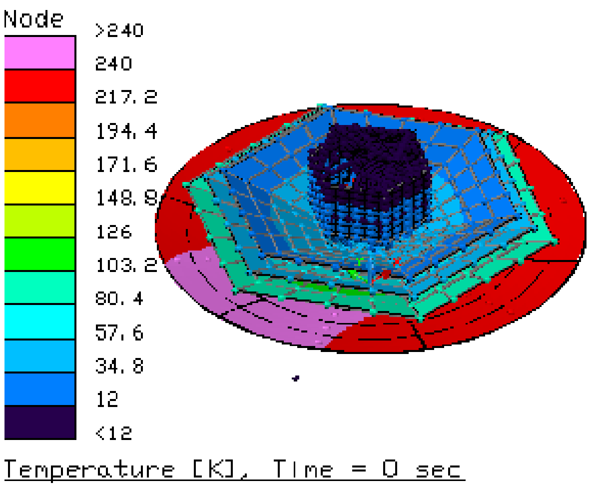

Figure 5: 3D color map of the temperature of EPIC.

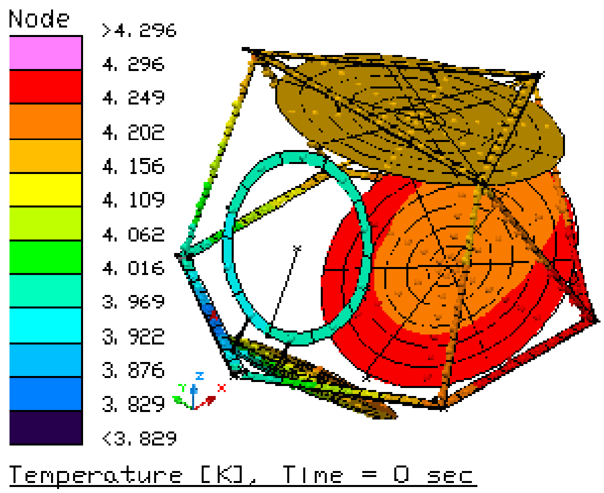

Figure 6: Color map of the Telescope.

Table IV: Heat transfer summary between different thermal stages.

	T(K)	Radiative Heat Transfer to Next Stage (W)	Conductive Heat Transfer to Next Stage (W)	Radiative Heat Transfer to Space (W)	Thermal Resistance to next stage (K/W)
1st Shield	231	78.5	3.91	16,300	29.4
2nd Shield	116	5.89	1.02	75.42	54.9
3rd Shield	60	0.689	0.256	6.00	85.9
4th Shield	38	0.0420	0.0266	0.857	752
Optical Box	18	0.00282	0.01045	0.0294	1340
Telescope	4	NA	NA	-4×10^{-6}	NA

4.3 Spinning the Spacecraft (Four- Shield Option)

We have also explored the effect of rotating the spacecraft at 0.5 rpm. The primary result is that the temperatures become more uniform on the shields as expected. Before the spacecraft is rotated, there is a 118 K steady state temperature variation in the first shield. With the rotation, a 1.2 K peak-to-peak sinusoidal temperature variation remains at 0.5 rpm. In the second shield, this time dependent signal drops to 0.3 mK . Therefore the attenuation factor is ~4000 per shield. Beyond the second shield, the temperature variation in the model is limited by digitization noise, and the 0.5 rpm signal is not observable. However, using the attenuation factor of 4000 per stage, one can extrapolate to a temperature variation of 19 pico-K at the fourth shield.

4.4 Three- Shield Option, Cryocooler On

The 3-shield option is the same as the 4-shield option with the exception that the 4^{th} shield is removed. For this option, a smaller focal plane box is actively cooled to 4K. The area of the Focal Plane is also reduced to 27% of that of the 4-shield case. The telescope reaches a higher equilibrium temperature (22K) by passive cooling. Additionally the Focal Plane is shielded by two radiation shields – the Inner and the Outer Focal Plane Boxes. In operation, the Inner Radiation Box is cooled to 4 K by the cryocooler. The Outer Focal Plane Box is not connected directly to the cryocooler. It is indirectly cooled to 8 K by the struts which connect it to the Inner Radiation Box. The power dissipated by the ADR (8 mW) is applied to the Inner Radiation Box. The cooling power versus temperature at the Inner Focal Plane Box is given in Table V. For this option the required heat lift at the cryocooler is 10.6 mW, including 8 mW heat loads from the ADR. Figure 7a shows the telescope temperature of the three-shield option in comparison with that of the four-shield option shown in Fig. 7b.

Table V: Cooling power at the Inner Focal Plane Box versus temperature. The Outer FP Box is cooled to 18 K if it is above 18K. If it is below, no heat is applied. The shaded column is the load on the cryocooler.

Inner FP Box Cooling power (mW)	0	4	8	10	10.5	10.55	10.58	10.6
Inner FP Box T (K)	24.96	21.53	17.49	11.41	5.28	4.81	4.24	3.12
Outer FP Box P (mW) and T(K)	7.09 18	4.13 18	0.88 18	0 13.96	0 8.30	0 7.89	0 7.28	0 6.16

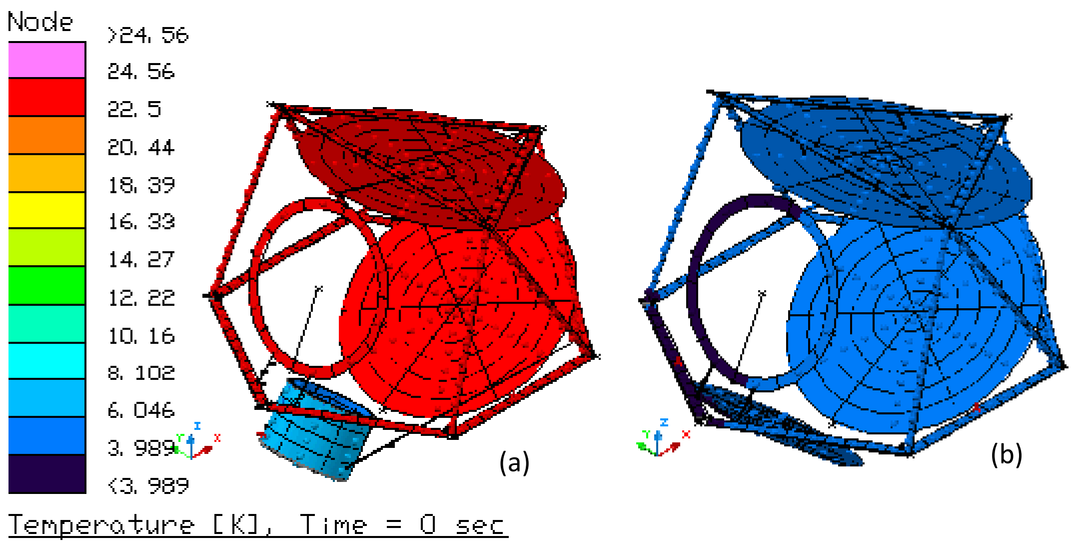

Figure 7: Telescope temperature for: (a) the three-shield option where only the Focal Plane Box is cooled to 4K, and (b) the four-shield option where the entire telescope is cooled to 4 K.

5. Conclusion

We have conducted a detailed thermal design of a sunshield and passive V-groove radiators for the EPIC mission. The designs presented in this paper will provide the necessary cooling for the mission. For the four-shield option, it reduces the heat lift at the 4 K stage of the cryocooler to 20.25 mW. For the three-shield option, this value is reduced to 10.6 mW. Cryocoolers with such heat lifts and operating at a base temperature of 4 K are within reach with current technology [5]. Future work includes fully modeling the double layered shields, and modeling the effect of non-grey radiative heat transfer between shields having large temperature differences [6].

6. Acknowledgment

The work carried out at the Jet Propulsion Laboratory, California Institute of Technology, was performed under a contract with the National Aeronautics and Space Administration.

7. References

[1] Bock J et al. 2009, "Study of the EPIC Intermediate Mission" arXiv 0906.1188

[2] Kelsall T, et al. "The COBE Diffuse Infrared Background Experiment Search for the Cosmic Infrared Background. II. Model of the Interplanetary Dust Cloud", Astrophysics Journal, 508:44-73 (1998).

[3] DiPirro M, "Cryogenic Technology for CMB-Pol: Passive Cooling and Stored Cryogen Systems" http://cmbpol.uchicago.edu/workshops/technology2008/depot/dipirro-passivecooling_revb.pdf

[4] Yorke HW et al., "Thermal Design Trades for SAFIR Architecture Concepts", Proc. SPIE Int. Soc. Opt. Eng., **5487**, 1617, 2004.

[5] Johnson DL, "Cryogenic Technology for CMB-Pol: Mechanical cryocoolers for the 4K to 200K temperature range"
http://cmbpol.uchicago.edu/workshops/technology2008/depot/johnson_cryocoolers.pdf

[6] Anderson KR, Paine C, "Non-Grey Radiation Modeling Using Thermal Desktop/SindaWorks" , paper 1009, Thermal and Fluid Analysis Workshop (TFAWS), Washington DC, August 9-11, 2006.
http://trs-new.jpl.nasa.gov/dspace/handle/2014/41071?mode=full